Analysis of the Yokeless and Segmented Armature machine

T.J. Woolmer, M.D. McCulloch
Oxford University, Engineering Department
Parks Road, Oxford, UK
OX1 3PJ

***Abstract*—This paper presents a new type of axial flux motor, the Yokeless And Segmented Armature (YASA) topology. The YASA motor has no stator yoke, a high fill factor and short end windings which all increase torque density and efficiency of the machine. Thus, the topology is highly suited for high performance applications. The LIFEcar project is aimed at producing the world's first hydrogen sports car, and the first YASA motors have been developed specifically for the vehicle. The stator segments have been made using powdered iron material which enables the machine to be run up to 300Hz. The iron in the stator of the YASA motor is dramatically reduced when compared to other axial flux motors, typically by 50%, causing an overall increase in torque density of around 20%. A detailed Finite Element analysis (FEA) analysis of the YASA machine is presented and it is shown that the motor has a peak efficiency of over 95%. Magnet segmentation and coating are shown to be particularly important in reducing the eddy current losses in the machine and it is shown that 4 magnet segments with an epoxy coating are an attractive option.**

I. Introduction

The Yokeless And Segmented Armature (YASA) topology is a new type of axial flux motor that shows a step change improvement in torque density and efficiency when compared to other axial flux motors. The topology is based around a series of magnetically separated segments that form the stator of the machine. The novel motor design is made possible by using powdered iron materials [1] that enable complex magnetic parts to be manufactured easily.

The motors have been developed for the LIFEcar project whose aim is to produce the world's first hydrogen sports car. The specific goals of the project are to create a "fun to drive" vehicle without compromising on efficiency. The specification for the LIFEcar project is four 300V drives that produce a peak torque of 360Nm and a top rotational speed of 1200 rpm. A 3:1 gearbox is being used on the output of each motor, so the peak toque and speed demand of the motors is 120Nm and 3600rpm. These specifications have been chosen to enable the vehicle to have impressive acceleration and regenerative breaking capabilities.

This paper begins with an overview of axial flux machines. The YASA topology is then presented and its design applied to the LIFEcar project. The LIFEcar YASA motor is then analysed using FEA to gain an accurate understanding of the electromagnet losses in the machine.

II. Axial Flux Machines

It is recognised in the literature that Axial Flux Permanent Magnet (AFPM) machines usually have higher torque densities and efficiencies that their radial flux counterparts [2]. Furthermore, the AFPM machine typically has a large aspect ratio which makes them of suitable dimensions for packaging in, or close to, each of the vehicle wheels. However, axial flux machines appear in the literature in many different topological forms, see Fig. 1 for two examples, as discussed by Aydin [3]. This is due to a number of different flux path options, coupled with different winding and magnet configurations.

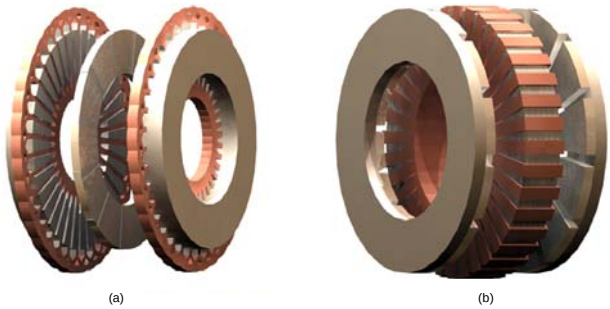

Fig. 1. (a) Internal rotor Axial Flux machine (b) Torus Axial Flux machine.

A study undertaken by Huang [4] compares the performance of two of the best performing axial flux machines, the NS Torus-S (lap) and the NN Torus-S topology. Huang observes that the NS Torus-S (lap) topology, Fig. 2(a) has a short stator yoke, increasing power density and reducing losses. However, a lap winding must be used for torque to be generated. Thus, the machine suffers from a poor fill factor and long end-windings which increases the outer diameter of the machine resulting in reduced power density and increased losses.

On the other hand, the NN Torus-S topology, Fig. 2(b) requires a large stator yoke to handle the flux from both rotors which increases losses and reduces power density. However, a back-to-back winding with high fill factor can be employed. This greatly reduces the protrusion of the end windings which

increases the power density and efficiency of the NN Torus-S type machine.

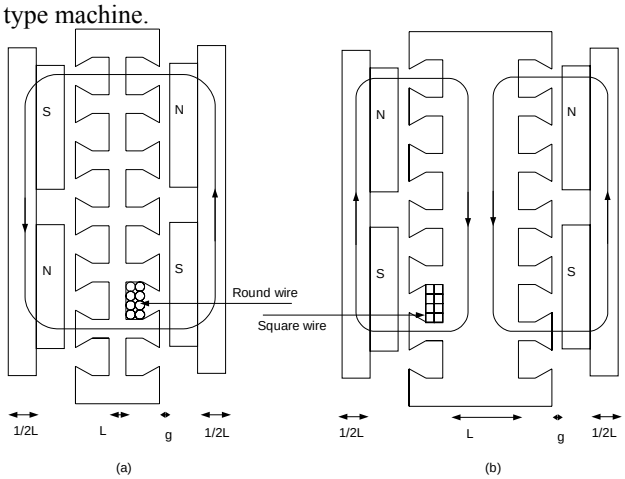

Fig. 2. (a) NS Torus-S (lap) machine (b) NN Torus-S machine

Overall, the machines have similar performance, although the NS Torus-S tends to have a slightly higher power density and peak efficiency.

III. The Yokeless And Segmented Armature Topology

No topology reported thus far combines the excellent winding characteristics of the NN Torus-S machine with the short stator yoke possible by using the NS Torus-S machine.

The YASA topology has been created to combine the positive characteristics of the NN Torus-S, and the NS Torus-S machine. The new topology is derived by manipulation of NS Torus-S machine, as follows:

1) Remove the stator yoke of the NS Torus-S machine. This can be done since the stator yoke of the NS Torus-S is not required for magnetic reasons, thus the teeth become magnetically unconnected.
2) Enlarge the pitch of the teeth so that their arc is similar to that of the magnets.
3) Wrap an individual winding around each of these teeth.
4) Join the teeth and windings together with high strength bonding material.

By following these steps, as shown in Fig. 3, the stator yoke has been completely removed saving weight and unnecessary iron losses. Furthermore, a simple coil with short end windings can be added to each tooth and by using square wire a high fill factor can be achieved.

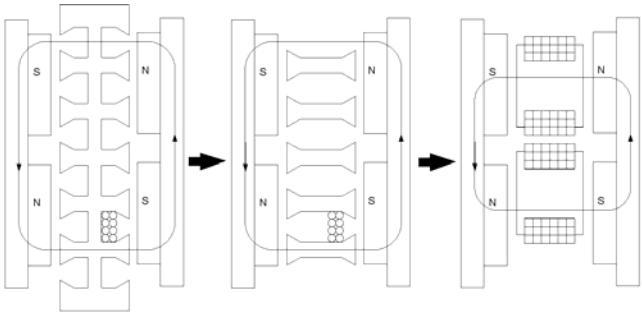

Fig. 3. Deriving the YASA topology

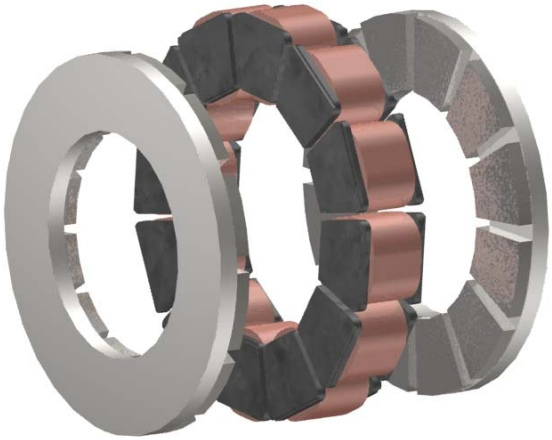

Fig. 4. The Segmented Armature Torus Topology

By making the steps above, a new topology of motor has been created that combines all the main advantages of the NN Torus-S and the NS Torus-S topologies. Fig. 4 shows a picture of the YASA topology. The increased power density and efficiency that the topology enables make it an ideal design for an electric vehicle. Sizing equations [6] suggest that typically the machine will have 50% less iron in the stator that the NN Torus-S machine.

IV. The LIFEcar Machine

A. YASA Machine Design

TABLE I
LIFEcar Machine Parameters

Machine Parameter	Symbol	Value	Unit
Number of Poles	p	10	
Number of Stator segments	N_{seg}	12	
Number of Phases	Q	6	
Phase resistance (50)	R	54	mΩ
Inductance	L	0.6	mH
Turns per segment	ns	37	
Conductor Width	w	2.2	mm
Conductor Height	h	2.2	mm
Outer Radius	R_o	102	mm
Inner Radius	R_i	66	mm
Shoe Length	L_{shoe}	5	mm

Bar Length	L_{bar}	30	mm
Active Length	L_{active}	79	mm
Airgap length	L_g	1.5	mm
Permanent Magnet Length	L_m	10	mm
Peak Current Density	J	16	A/mm^2
Active material weight		12	Kg
Peak Efficiency	η	>95	

The stator of the YASA motor is made by pressing Soft Magnetic Composite (SMC) materials [1], [6] produced by Höganäs. The stator iron shown in Fig. 4 was manufactured in 3 parts: 2 shoes and central bar. The parts were bonded together and wound to create the stator segments shown in Fig. 4.

The static design of the LIFEcar motor was undertaken using firstly sizing equations, and then refined using static FEA. The FEA showed that an outer diameter of 204mm was required to give 120Nm of torque. K_r (the ratio of outer to inner diameter) has been chosen as 2/3 [6] so the inner diameter is 136mm. The 10 pole 12 tooth configuration was chosen to optimise weight and performance [6]. The electrical machine parameters are shown in Table 1.

Fig. 5 shows the flux densities within the motor during no load and peak load conditions. The no load air gap flux density is just over 1T, which has been achieved by using large NdFeB magnets. The motor bars have been designed to carry a no load flux of 1.5T, as shown in Fig. 4b. At peak load the flux density within the bars increases to 1.8T, but stays within the 2T saturation limit of the SMC material.

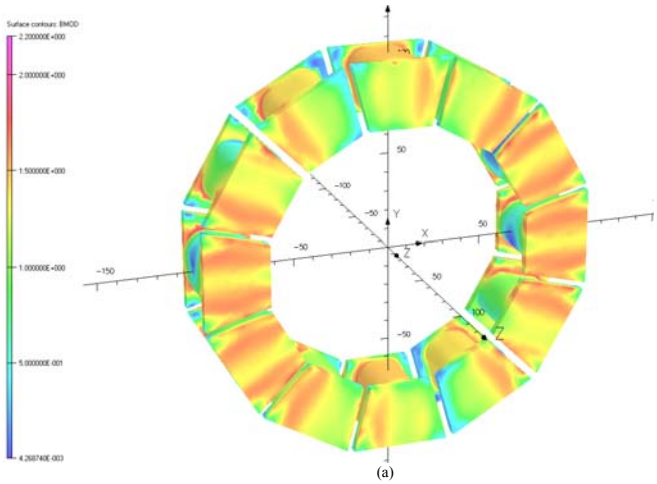

(a)

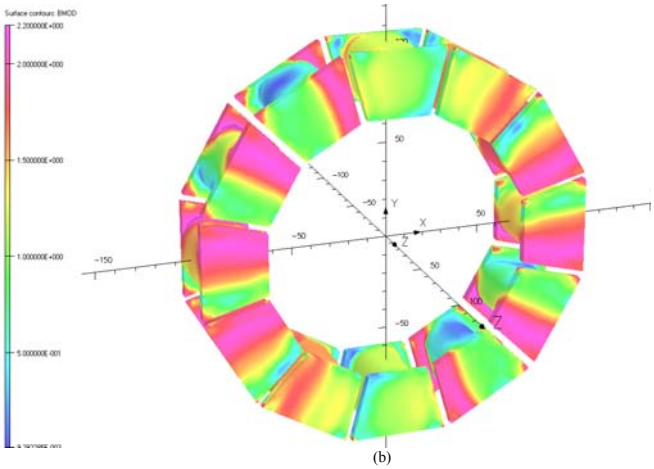

(b)

Fig. 5. Flux densities within the YASA: (a) under no load, (b) at peak load

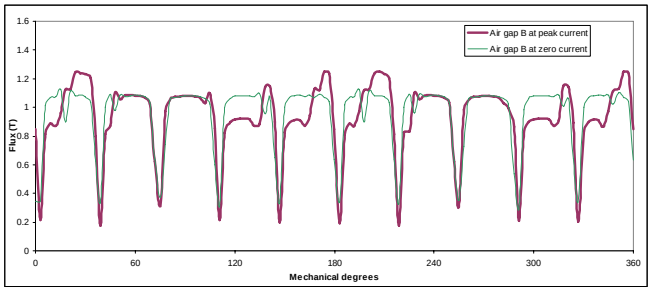

(a)

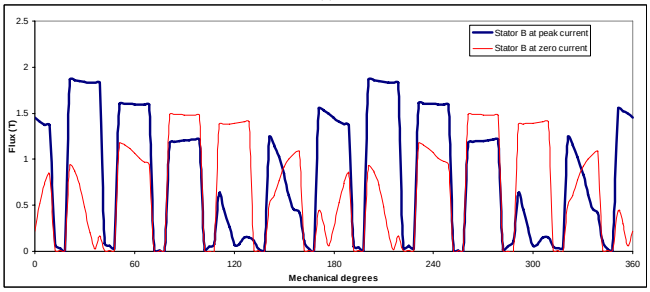

(b)

Fig. 6. Flux densities within the YASA motor (a) air gap (b) in the stator bars at peak load and no load

B. *Machine Losses – Static Analysis*

Machine losses are a complex function of speed and torque. Electromagnetic losses occur in two ways: magnetic hysteresis and I^2R losses. The I^2R can be broken down into two distinct groups, losses in the motor coils and induced eddy current losses. The motor I^2R coil losses can be calculated from the estimated coil resistance and the torque-current profile of the motor from the static analysis.

The measured resistance of 1 phase of the machine at 50˚C is 0.054Ω. Using the estimated current densities required to achieve different values for torque, the copper losses for three torque conditions are given in Table 1.

TABLE II
COPPER LOSSES

Torque (Nm)	Total Current (A)	Loss (W)
10	13.6	10.0

40	54.4	159.9
120	163.3	1439.4

The static analysis can also be used to calculate the magnetic hysteresis losses using a combination of simulation results and information about the materials from the manufacturer. The hysteresis losses in the stator are directly proportional to the speed of the motor and weakly coupled to motor toque. The loss data for Somaloy 3P, Fig. 7(a), has been extrapolated using the least squares method so that the hysteresis loss can be accurately predicted for the shoes and bar in the machine under different loading conditions.

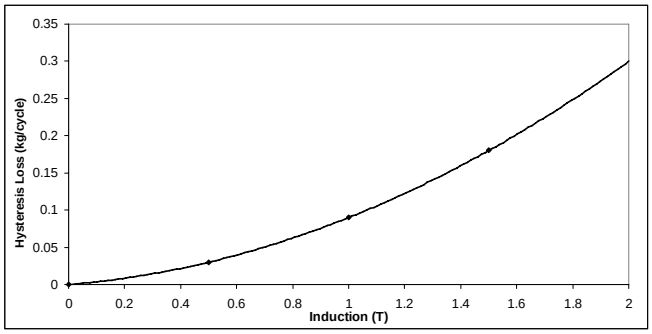

(a)

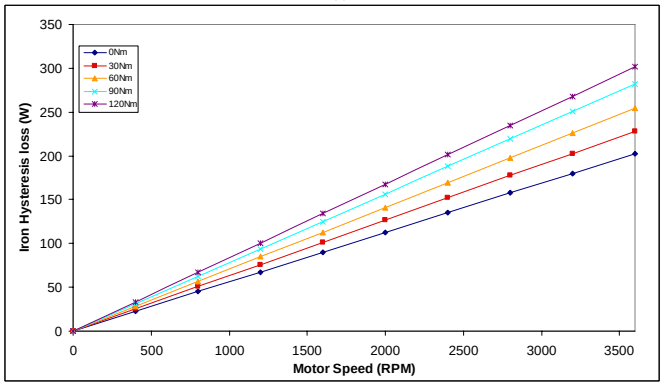

(b)

Fig. 7. (a) Loss in Somaloy 3P/kg at 1 Hz as a function of flux density, (b) Hysteresis losses in the stator iron

Fig. 7(b) shows the sensitivity of the SMC hysteresis losses to motor load and speed. As the loading of the motor is increased, the armature current increases the peak flux in the stator iron, as shown in Fig. 8. This means that the peak loading condition will have a 40% increase in hysteresis losses compared to the no load condition. However, the peak loading conditions only last for 5-10s so the extra heat produced from the additional hysteresis loss will not be significant.

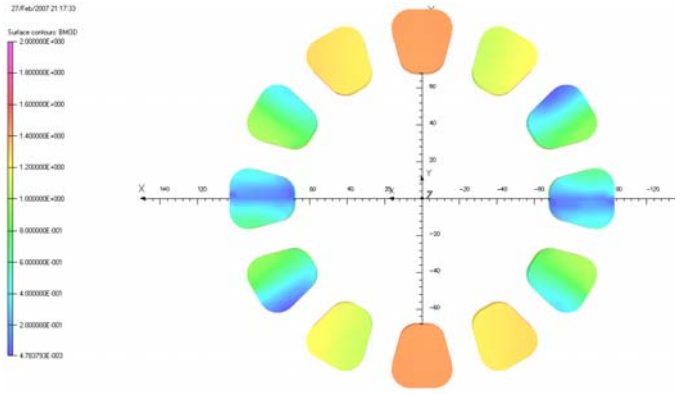

(a)

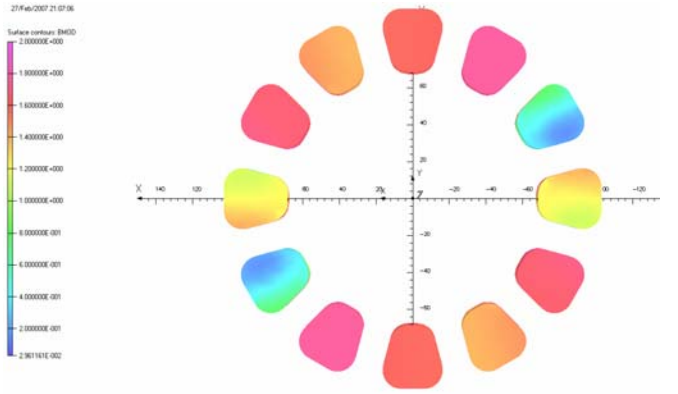

(b)

Fig. 8. Flux density distribution at the centre of the bars at (a) half load and (b) peak load

C. *Stator Eddy Currents*

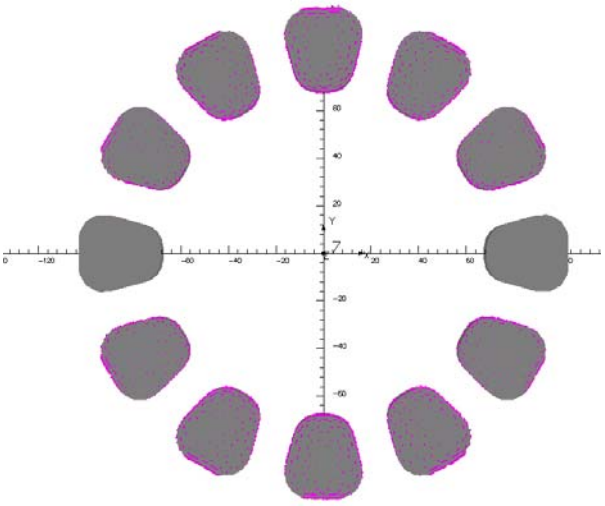

(a)

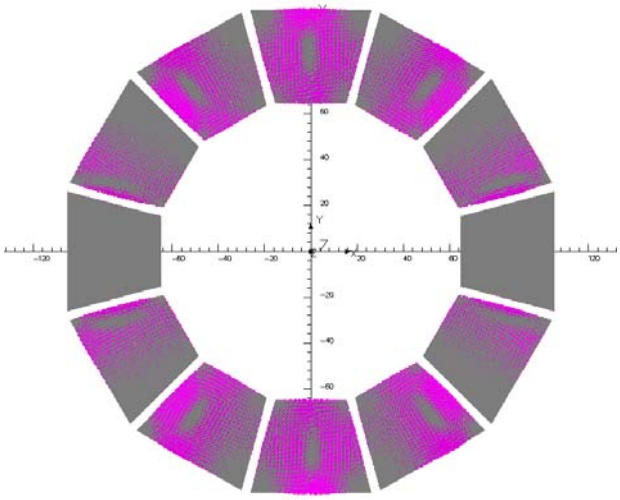

(b)

Fig. 9. Eddy current distribution in (a) the shoes and (b) bars of the stator at 3600 rpm

To calculate the eddy current losses accurately within the electrical machine a time stepping finite element method is required. The Carmen solver, part of the Opera 3D finite element package [7] has been used to achieved this. Stator eddy currents are produced by time varying magnetic fields from the rotor inducing eddy currents in stationary conductors.

The most significant eddy currents in the stator are those induced in the stator iron, since it observes the largest changing flux density. However, the motor casing and copper winding are also affected by eddy currents, but to a lesser degree.

The powdered iron material used in the machine has a relatively high electrical resistivity of 400μΩm. The induced eddy currents in the shoes and bars of the machine are shown in Fig. 9. Despite the high resistivity of the SMC material, the high machine electrical frequency (300Hz) and large area for eddy current paths mean that there are significant losses caused by eddy currents. The losses for the stator and casing are plotted in Fig. 10 as a function of speed for the no load and peak load conditions. It should be noted that with the exception of the no load case, the losses in the stator will actually be greater that those shown in Fig. 10 since the losses were calculated by time stepping the rotor for a fixed commutation position.

The eddy currents in the stator add a significant extra loss to cruise speed of the vehicle. One possible method of reducing the stator eddy currents is to add a lamination to the shoes or bars. Another is to use a material with higher resistivity. However, neither of these solutions are thought to be practical for the LIFEcar project.

D. Rotor Eddy Currents

The rotor eddy currents are caused by the interaction between the stationary field of the stator and the movement of the rotor through that field. NdFeB magnets have a conductivity of approximately 16000μΩm, approximately 10 times less than mild steel, which can lead to a significant heating affect of the magnets. Reducing this heating affect is important, not only because the magnets have a maximum working temperature of 180˚C, but also because the energy product of the magnets is significantly reduced as their temperature is increased.

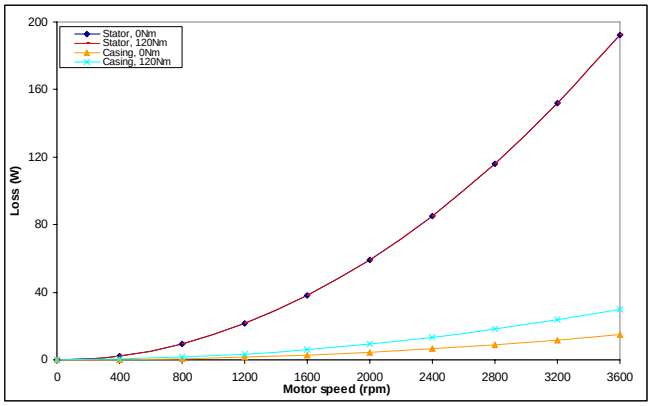

Fig. 10. Eddy losses in the stator and casing at zero and peak torque

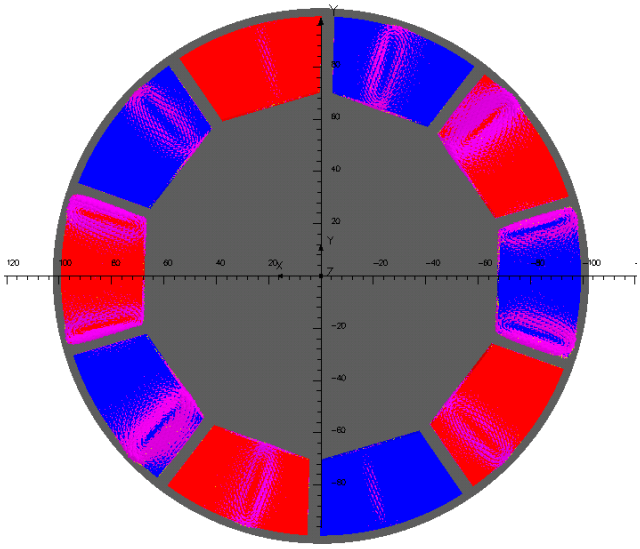

(a)

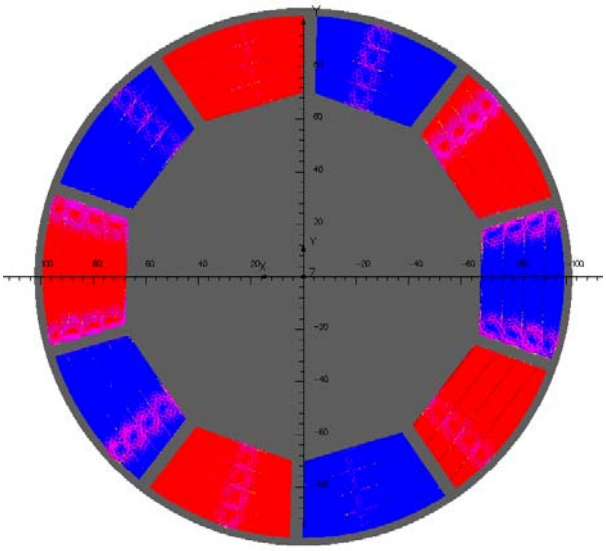

(a)

Fig. 11. (a) No magnet laminations (b) Three laminations

Table 3 presents seven rotor design options that have been analysed. Design 1 used nickel coated NdFeB magnets attached to a mild steel back iron. The electrical short circuit between the magnets and the back iron causes large eddy currents to travel between the magnets and the back iron, significantly increasing the rotor losses. By changing the magnet coating to epoxy, the magnets become electrically isolated from the back iron, significantly reducing the magnet and back iron losses. To further reduce the losses in the magnets it is necessary to add laminations that cut the eddy current paths. Fig. 11 show the eddy current paths for no laminations and 3 laminations.

TABLE III
ROTOR LOSSES

	Laminations	Mag. Coating	Magnet loss (W)	Iron loss (W)	Loss (W)
Design 1	0	nickel	864	522	1386
Design 2	0	epoxy	548	64	612
Design 3	1	epoxy	268	64	332
Design 4	2	epoxy	157	64	221
Design 5	**3**	**epoxy**	**104**	**64**	**168**
Design 6	4	epoxy	75	64	139
Design 7	5	epoxy	54	64	118

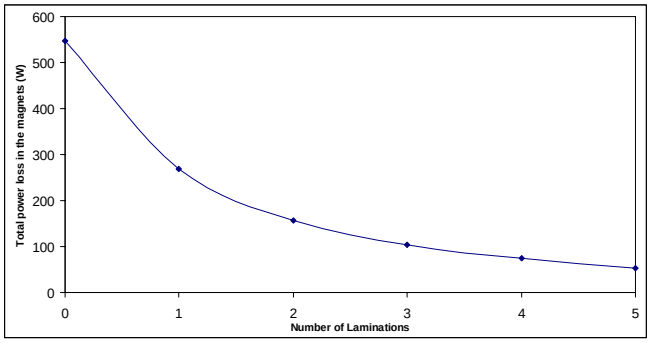

Fig. 12. FEA magnet losses as a function of lamination number

The advantage of adding laminations to the magnets is shown in Fig. 12. Adding three laminations reduces the magnet losses by a factor of five and this design has been chosen for the LIFEcar motors. The benefit of increasing the number of laminations beyond three was not thought to be worthwhile since the extra reduction in losses incurs a significant manufacturing cost penalty.

E. LIFEcar efficiency map

The electromagnetic loss data presented in this section has been compiled to form an efficiency map, see Fig. 13. The peak efficiency of the motor is just over 96% and occurs between 3200 to 3600rpm and 50-60Nm. The 80mph cruising speed which requires an output of 5kW per motor is achieved at 92%.

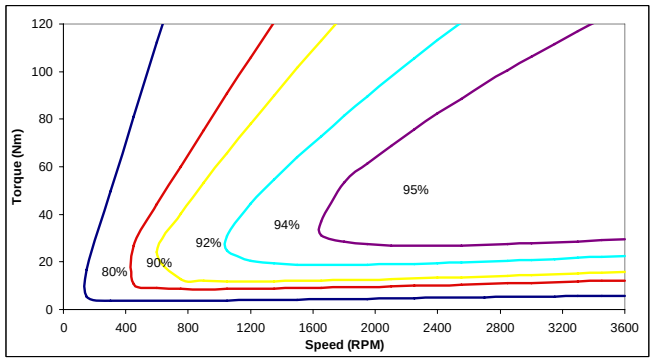

Fig. 13. Efficiency map of the YASA motor

V. CONCLUSIONS

The YASA motor presented in this paper has a higher torque density than other axial flux machines, typically by 20%. Furthermore, the iron in the stator is reduced by around 50%. The motor has been derived from the NS Torus-S topology by removing the stator yoke, enlarging the pitch of the teeth and wrapping a winding around each of the individual teeth.

Finite Element analysis has been used to accurately calculate the machine losses for the LIFEcar YASA machine. The results have shown that SMC material produced by Höganäs performs well, although significant eddy currents add to the overall losses at electrical frequencies about 250Hz.

One possible technique to reduce these eddy currents is to laminate the SMC segments radically.

FEA has also revealed that magnet segmentation and coating are particularly important for controlling the rotor losses. An epoxy coating will significantly reduce rotor losses since it stops eddy current paths between the magnets and back iron.

ACKNOWLEDGEMENT

The authors would like to thank Höganäs for their support on this project and the DTI for their generous funding.

REFERENCES

[1] http://www.hoganas.com accessed February 07

[2] K. Akatsu et al, "A comparison between Axial and Radial flux-motors PM motors by Optimum Design Method from the required output NT characteristics", *Int. Conf. Electrical Machines*, pp1611-1618, 2004

[3] M. Aydin, S. Huang and T.A. Lipo, "Axial Flux Permanent Magnet Disc Machines: A Review", *In Conf. Record of SPEEDAM*, pp. 61-71, May 2004,

[4] S. Huang, M. Aydin, and T.A. Lipo, "TORUS Concept Machines: Pre-Prototyping Assessment for Two Major Topologies". *Int. Conf. Rec. IEEE IAS* Annual Meeting, Chicago, pp. 1619-1625, Oct. 2001.

[5] F. Magnussen, P. Thelin and C. Sadarangani, "Design of Compact Permanent Magnet Machines for a Novel HEV Propulsion System", *Electric Vehicle Symposium 20 (EVS)*, Long Beach, USA, November 2003.

[6] Woolmer, T, and M. McCulloch, "Axial flux Permanent Magnet Machines: A new topology for high performance applications", Hybrid Conference, Warwick, UK December 2006.

[7] http://www.vectorfields.com accessed February 07